Research Article

Tao Meng*, Songsong Lian, Kanjun Ying, and Hongming Yu

Feasibility study of cement-stabilized materials using 100% mixed recycled aggregates from perspectives of mechanical properties and microstructure

https://doi.org/10.1515/rams-2021-0031
received March 08, 2021; accepted April 19, 2021

Abstract: The research on the highly efficient reutilization of mixed recycled aggregates (MRA) produced from construction and demolition waste has attracted significant attention globally. In this study, the feasibility of using 100% MRA in cement-stabilized materials was investigated. The mechanical properties and microstructures of cement-stabilized MRA (CSMRA) materials containing 100% MRA were systematically examined through unconfined compressive strength (UCS) test, indirect tensile strength (ITS) test, drying shrinkage test, X-ray diffraction analysis, mercury intrusion porosimetry, and scanning electron microscopy. Results showed that the UCS and ITS of CSMRA materials were significantly enhanced with the increase of cement content and curing age, and there was almost a linear relationship between the UCS and ITS. The failure behavior of CSMRA materials under load showed three typical stages: compaction stage, elastic stage, and yield stage. The increase of the cement content caused the drying shrinkage deformation of CSMRA to increase sharply when the cement content exceeded 4%. The microstructural analysis indicated that cement had both filling and binding effects on CSMRA materials. The strength growth with cement content and curing age was because of the constant hydration of cement minerals, producing more calcium silicate hydrate binders between aggregates. Moreover, the increasing cement content could reduce the porosity and optimize the pore structure distribution of CSMRA materials. The findings of this study demonstrate that the use of 100% MRA in cement-stabilized materials as a road base is feasible, which will significantly enhance the utilization efficiency of MRA.

Keywords: mixed recycled aggregates, cement-stabilized materials, mechanical properties, microstructure

Abbreviations

MRA	mixed recycled aggregates
CSMRA	cement-stabilized MRA
UCS	unconfined compressive strength
ITS	indirect tensile strength
XRD	X-ray diffraction
MIP	mercury intrusion porosimetry
SEM	scanning electron microscopy
C_2S&C_3S	calcium silicate
CSH	calcium silicate hydrate
Aft	ettringite

1 Introduction

Advancements in urban development have led to the demolition of several old buildings, which resulted in large quantities of construction and demolition waste (C&DW) [1]. Over 10 billion tons of C&DW are generated worldwide each year, among which China produces approximately 2.3 billion tons, the European Union produces over 900 million tons, and the United States produces 500 million tons [2,3]. The generation of such vast amounts of C&DW without adequate management will cause adverse impacts on the environment, including landfill depletion, greenhouse gas emission, and water

* **Corresponding author: Tao Meng,** College of Civil Engineering and Architecture, Zhejiang University, Hangzhou 310058, China, e-mail: taomeng@zju.edu.cn
Songsong Lian, Kanjun Ying: College of Civil Engineering and Architecture, Zhejiang University, Hangzhou 310058, China
Hongming Yu: College of Civil Engineering and Architecture, Zhejiang University, Hangzhou 310058, China; Hangzhou Xincheng Dinghong Real Estate Development Co., Ltd., Hangzhou 310058, China

pollution [4–7]. Thus, there is an urgent need to dispose and recover C&DW reasonably.

Several studies have been conducted on the reuse and recycling of C&DW in infrastructural construction projects [8–11]. After crushing and sieving C&DW, the particles can be used as mixed recycled aggregate (MRA), whose composition mainly includes concrete, bricks, mortar, glass, wood chips, and some hazardous impurities [12–14]. The mechanical properties of MRA are complex owing to its various components, and the components of MRA from different regions may have significant differences [15–18]. Therefore, it is difficult to reuse MRA efficiently as a conventional recycled concrete aggregate. Only 20–30% of MRA is recovered globally [19], and the utilization rate of MRA in China is limited to less than 10% [20].

Cement-stabilized aggregate materials, which are compacted mixtures of aggregate, cement, and water, have been widely used as road base and sub-base pavements in many countries [21–23]. Recently, several scholars have considered using recycled aggregates as an alternative to natural aggregates in cement-stabilized materials to preserve natural aggregates and reduce environmental pollution from construction waste [24–29]. Most previous studies focused on the feasibility and evaluation the mechanical strength of cement-stabilized recycled aggregates. For example, Leite et al. found that the compaction process resulted in partial crushing and disintegration of recycled aggregates, modifying the grain-size distribution through bearing capacity and repeated load triaxial tests. This physical change made the recycled aggregates denser to improve their bearing capacity, resilient modulus, and permanent deformation; thus, they may be utilized as a base layer for low-volume roads [30]. Mohammadinia et al. evaluated the geotechnical properties of cement-treated recycled aggregate materials by the laboratory experiment [31,32]. A numerical model has been developed to simulate the macro- and micro-mechanical properties of lightly cement-stabilized recycled concrete aggregates under unconfined compression [31,32]. Hou et al. investigated the mechanical strengths of cement-stabilized recycled concrete aggregates and established strength development equations and relation models of mechanical indexes [33]. Xuan et al. studied the effects of quality and variation of recycled masonry on cement-stabilized materials [34,35]. They found that the decreasing masonry content and the increasing cement content could increase the unconfined compressive strength (UCS) and rebound modulus; in addition, the indirect tensile strength (ITS) of cement-stabilized materials without masonry was twice of that with 100% masonry [34,35]. They also determined the deformation behavior of cement-treated demolition waste with recycled masonry and concrete. Results showed that the masonry content and cement content were the dominating factors affecting drying shrinkage and thermal expansion [36].

Furthermore, several researches focused on the practical engineering applications of cement-stabilized recycled aggregate base. Jia et al. determined the engineering properties of recycled C&DW in the application of low-volume roads in rural areas in China [37]. Agrela et al. utilized cement-stabilized recycled aggregates materials as road base in an actual project in Malaga, Spain. Compared with natural aggregates, recycled aggregates may result in the weakening of workability of cement-stabilized materials due to the high water absorption [38,39].

Although various studies related to the reuse of recycled aggregates in cement-stabilized materials for road base and sub-base pavements have been carried out, most recycled aggregates used in these studies were recycled concrete aggregates or concrete components of MRA. Besides, researchers only used 10–70% MRA to prepare the cement-stabilized materials, and few researchers have studied the feasibility of using 100% MRA in cement-stabilized materials. The lack of systematic research on cement-stabilized MRA (CSMRA) limits the practical application of MRA as road bases.

The objective of this study is to investigate the feasibility of cement-stabilized materials produced with 100% MRA as road base layer. Hence, the strength, dry shrinkage properties, and failure behavior of CSMRA materials produced with 100% MRA were examined. In addition, microstructural analyses such as X-ray diffraction (XRD), mercury intrusion porosimetry (MIP), and scanning electron microscopy (SEM) were used to determine the effects of the cement content and curing age on CSMRAs. This article aims to realize the large-scale and high-valuable utilization of MRA in the road foundation, which promotes the utilization of construction demolition waste and alleviates the shortage of construction resources.

2 Experiment

2.1 Materials

The MRA utilized in this study was produced by Hangzhou Qianjiang New City Municipal Garden Construction Co., Ltd. In the plant, large quantities of CD&W, which were derived from the renovation and demolition of old buildings and structures located in Zhejiang Provinces China,

Figure 1: MRA: (a) 0–9.5 mm fine aggregates and (b) 9.5–31.5 mm coarse aggregates.

were crushed and sieved to MRA with different particle sizes. As shown in Figure 1, 0–9.5 mm fine size and 9.5–31.5 mm coarse size of MRA were used for the experimental tests.

The main composition of MRA with different particle sizes (≥2.36 mm) is displayed in Figure 2. The MRA mainly contained concrete rocks, crushed bricks, ceramic tiles, and wood chips, which accounted for 61.3, 31.7, 6.6, and 0.4% of the total weight, respectively. The particle size distribution of concrete rocks, crushed bricks, ceramic tiles, and wood chips was concentrated into 9.5–31.5 mm, 4.75–26.5 mm, 9.5–26.5 mm, and 2.36–16.0 mm, which meets the difficulty degree of being broken. Figure 3 shows the particle size distribution of MRA. Table 1 presents the main mechanical properties of fine and coarse size MRA. Because of its complex components, MRA had a lower apparent density and significantly higher water absorption, flakiness content, and crushing index than that of conventional natural aggregates required by GB/T 14685-2011.

P O 42.5 cement manufactured by Hangzhou Fuyang Qianchao Cement Co., Ltd. and tap water were used in

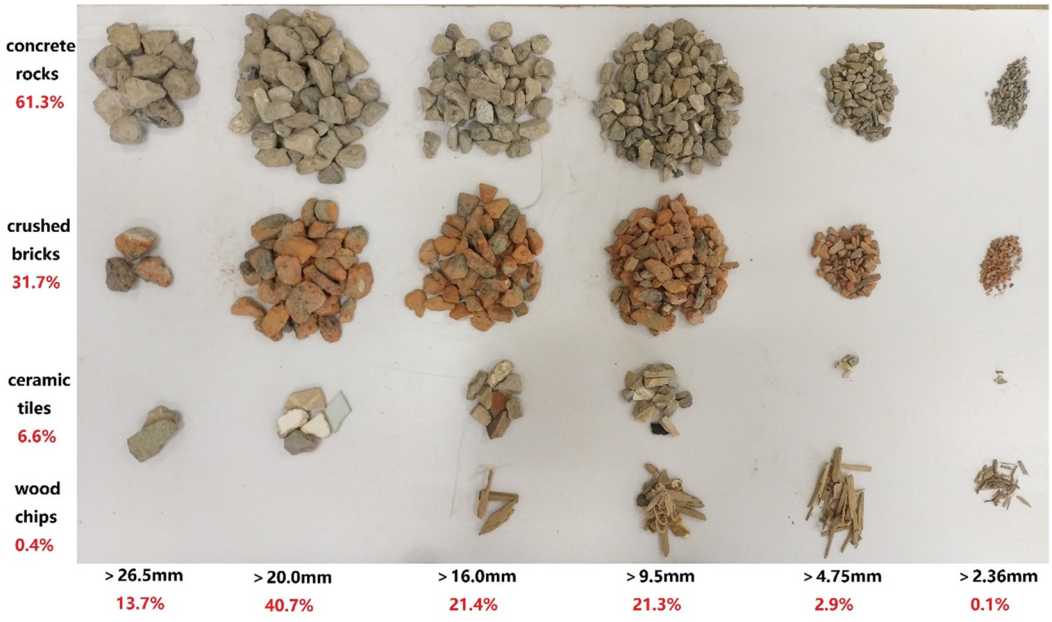

Figure 2: Main composition of MRA.

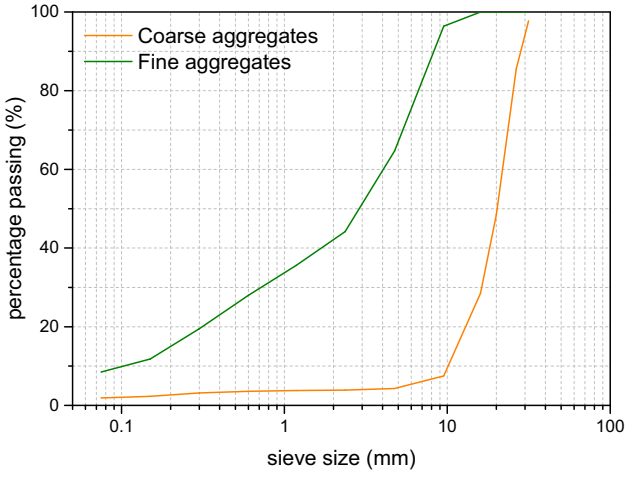

Figure 3: Particle size distribution of MRA.

this study. The chemical and mineral compositions of cement are presented in Tables 2 and 3, respectively.

2.2 Mixture

The coarse and fine aggregates were combined at a ratio of 1:1.2 to prepare the cement-stabilized materials gradation as stated in Specifications for Design of Highway Asphalt Pavement (JTG D50-2017) [40]. The final aggregate gradation curves of CSMRA materials are shown in Figure 4.

Cement contents of 0, 3, 4, 5, and 6% of MRA in mass were selected. The water content was determined according to compaction test guidelines specified in the Test Methods of Materials Stabilized with Inorganic Binders for Highway Engineering (JTG E51-2009) [41]. The optimum water content could be estimated from the curve of water content–dry density relationship, as shown in Figure 5, to ensure that the compactness of CSMRA materials was maintained. The mixing ratios of CSMRA materials are listed in Table 4.

2.3 Sample prepping and curing

By following the specifications of the Standard JTG E51-2009 [39], the MRA, water, and cement were gradually

Table 2: Chemical composition of cement

Composition	Al_2O_3	SiO_2	CaO	Fe_2O_3	SO_3	MgO	f-CaO
wt%	4.36	22.37	61.08	3.38	2.45	2.43	0.86

Table 3: Mineral composition of cement

Composition	C_3S	C_2S	C_3A	C_4AF
wt%	56.47	20.72	6.17	10.4

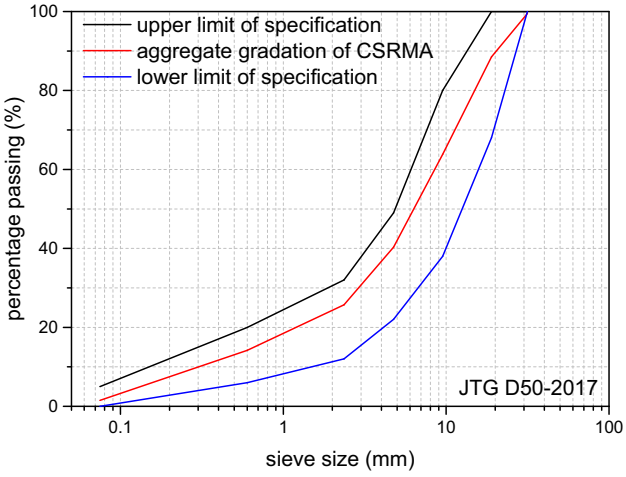

Figure 4: Aggregate gradation of CSMRA materials.

added into a mixer and mixed thoroughly for 3 min. The mixture was then poured into steel moulds and compacted to form Φ100 ± 2 mm × H100 ± 2 mm cylinder specimens for strength tests and 100 ± 2 mm × 100 ± 2 mm × 400 ± 5 mm cuboid specimens for drying shrinkage tests. The mixture was compacted in three layers with 25 blows per layer with an automatic compactor after placed in the mould. Except for the C0 group, the cylinder specimens were cured for 3, 7, 14, and 28 days, while the cuboid specimens were cured for 7 days under room conditions at 20°C temperature and 95% relative humidity. The specimens of C0 group were cured at 20°C temperature and 60% relative humidity because they could not be formed under high humidity.

Table 1: Mechanical properties of fine and coarse size MRA

Properties	Apparent density ($kg \cdot m^{-3}$)	2 h water absorption (%)	24 h water absorption (%)	Flakiness content (%)	Crushing index (%)
Fine aggregates	2,560	19	21	8	32
Coarse aggregates	2,469	8.3	8.5	15	33

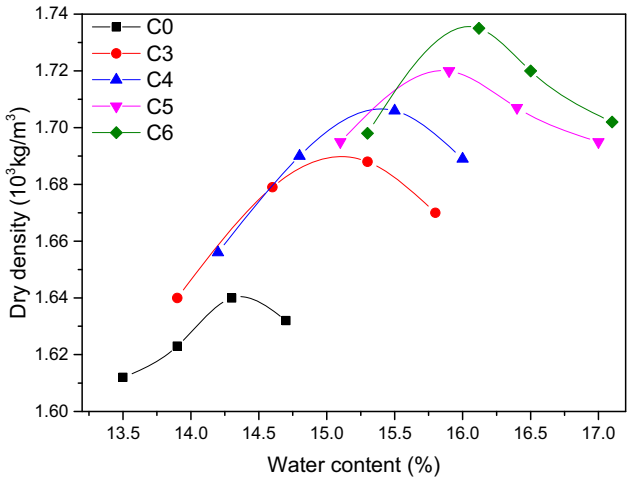

Figure 5: Relationship between water content and dry density.

Table 4: Mixing ratios of CSMRA materials

No.	MRA	Cement	Water
C0	100	0	14.3
C3	100	3	15.3
C4	100	4	15.5
C5	100	5	15.9
C6	100	6	16.1

2.4 Testing procedures

2.4.1 UCS and ITS

The cylinder specimens were removed from the curing room after curing for the specific ages and wiped using a dried towel. Nine specimens were tested for both UCS and ITS tests according to JTG E51-2009. A hydraulic testing machine with a maximum loading of 100 kN and a minimum range of 0.01 kN was produced by Jinan Meters Testing Technology Co., Ltd. and used for UCS and ITS tests. The loading rate was approximately 1 mm·min^{-1}. During the loading process, the vertical and horizontal displacements of specimens were recorded by extensometer. UCS and ITS in MPa were estimated using the following equation: UCS = $4P/\pi D^2$, ITS = $2P/\pi hD$, where P is the ultimate load (N), h is the sample height (mm), and D is the diameter of the sample (mm).

2.4.2 Drying shrinkage properties

After curing for 7 days, three cuboid specimens for each group (except C0 group) were kept in a room at 20°C temperature and 60% relative humidity for drying shrinkage tests. The drying shrinkage deformation and weight loss of each specimen within 31 days were measured by dial

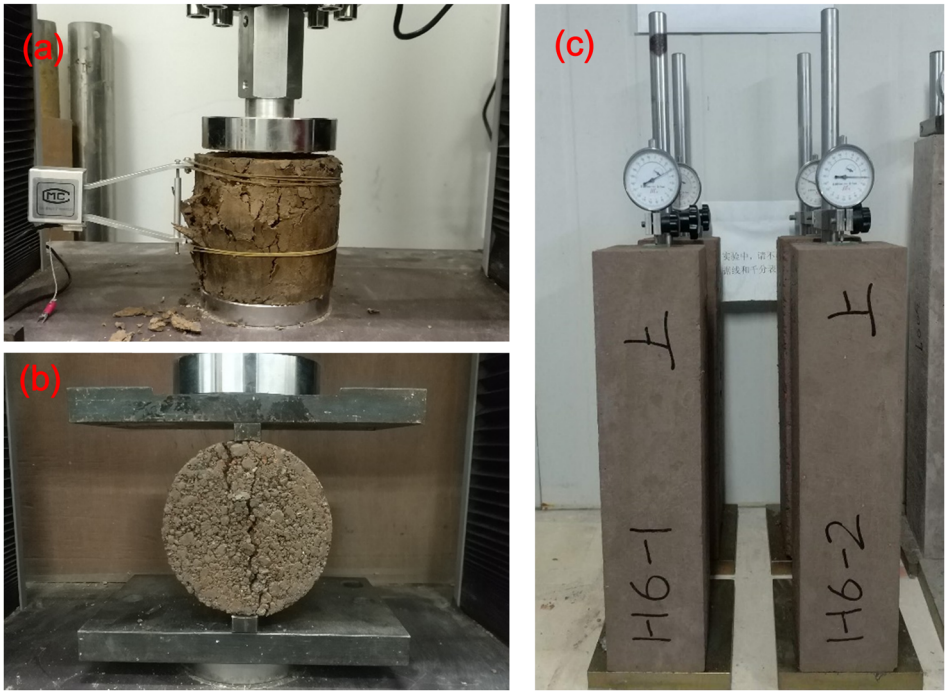

Figure 6: Test devices used for (a) UCS, (b) ITS, and (c) drying shrinkage tests.

gauge and electronic scale, respectively. The test devices used for the UCS, ITS, and drying shrinkage tests are shown in Figure 6.

2.4.3 XRD

The specimens for the XRD analysis were broken into tiny fragments after the UCS tests were performed, and particles of cement mortar were picked and ground to a residue ratio on the 80 μm sieve less than 2% at specific curing time. Bruker D8 ADVACNCE X-ray diffractometer from Bruker company, Germany, was used for the XRD analysis. CuKa radiation source, scanning angles of 10–80°, step length of 0.026°, and acceleration voltage of 40 kV were applied in this experiment.

2.4.4 MIP

The micro pore structures of CSMRA materials were determined through the MIP test. The specimens for MIP were broken into small pieces with a size of 3 mm × 3 mm × 3 mm and dried at 60°C for 24 h after conducting the UCS tests. The mercury analyzer used for this experiment was an AutoPore IV9510 automatic mercury porosimeter manufactured by McMurraytic Instruments Co., Ltd, USA.

2.4.5 SEM

The specimens used for SEM were disintegrated into small pieces, and the hydration process was stopped by pure alcohol at a specific age. Those small pieces were sprayed with gold for 60 s in SBC-12 small particles sputtering apparatus to make specimens conductive. Microscopic structures of specimens under different magnifications were observed with FEG-650 Quanta field emission environment scanning electron microscope produced by ThermoFisher Scientific Company, USA.

3 Results and discussion

3.1 Mechanical strength

Figure 7 shows the UCS and ITS results of CSMRA materials with different cement contents at 3, 7, 14, and 28 days. It can be found that the UCS values of C0 group at 3, 7, 14, and 28 days were 0.18, 0.20, 0.21, and

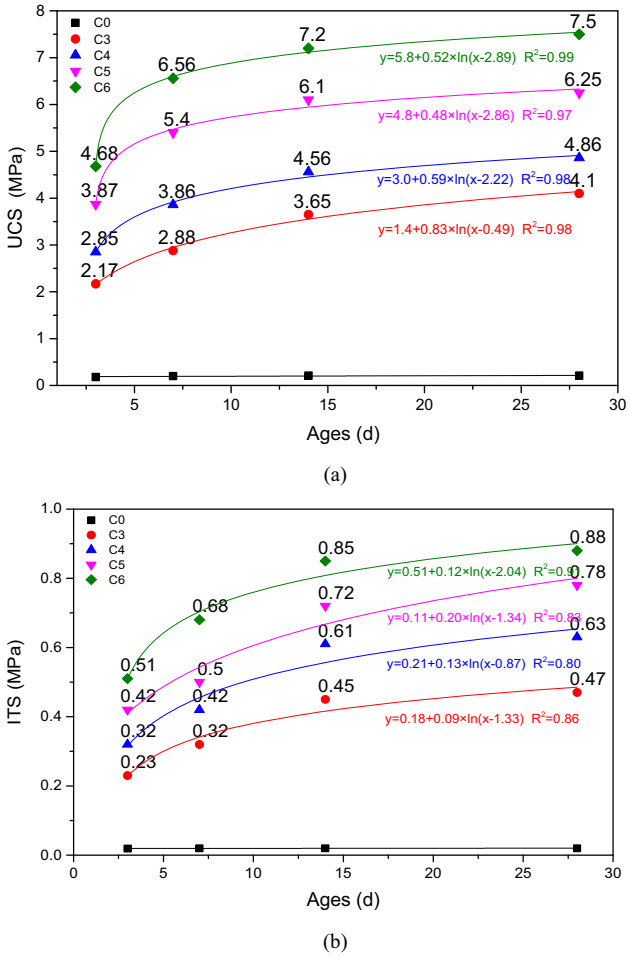

Figure 7: (a) UCS and (b) ITS of CSMRA materials with different cement contents.

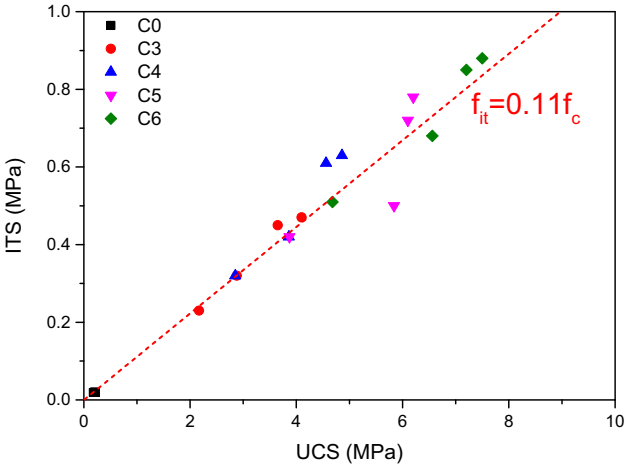

Figure 8: Relationship between UCS and ITS of CSMRA materials.

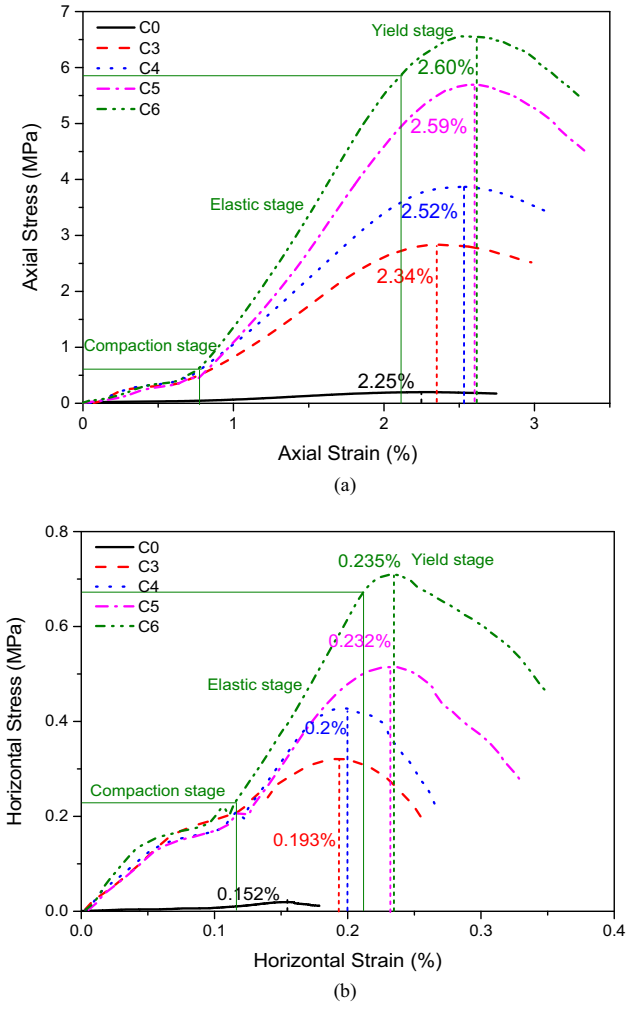

Figure 9: Stress–strain curve of (a) unconfined compressive and (b) indirect tensile tests of CSMRA materials at 7 days.

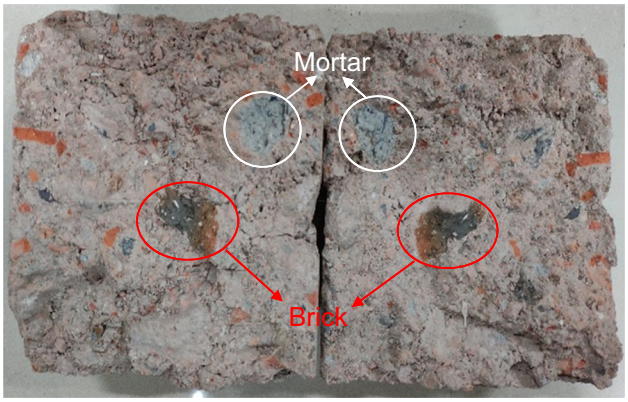

Figure 10: Failure surface of CSMRA specimens after indirect tensile test.

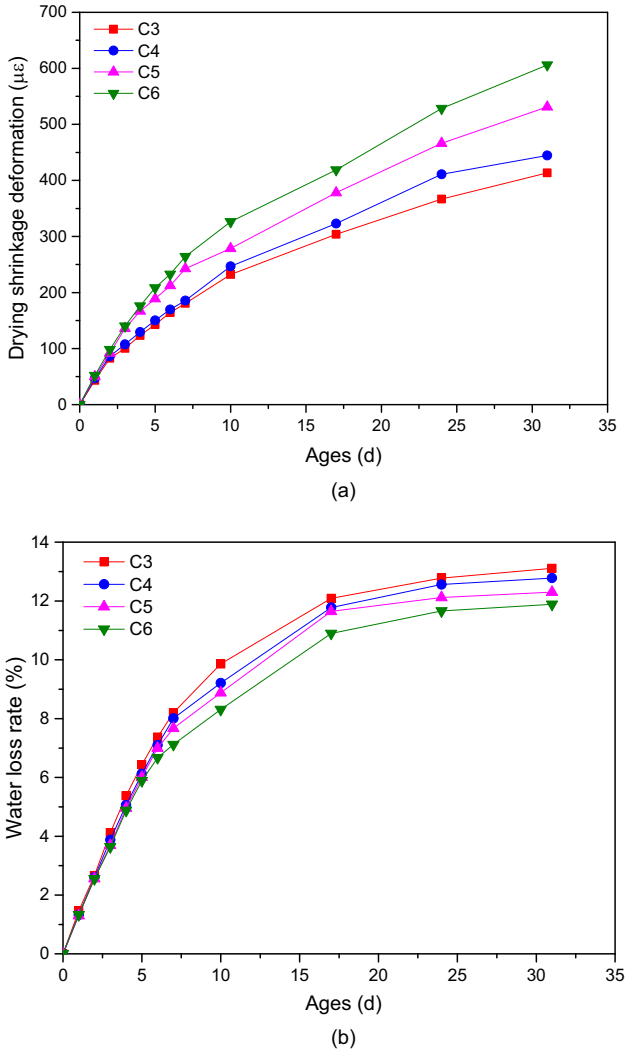

Figure 11: (a) Drying shrinkage deformation and (b) water loss rate of CSMRA materials with different cement contents.

0.21 MPa, respectively. The ITS of C0 group was only 0.02 MPa. It indicated that the strength of CSMRA materials was very low and hardly increased with curing ages when no cement stabilizer was present in the specimens. However, the UCS and ITS values for the C3, C4, C5, and C6 groups were significantly higher and increased with age due to the constant hydration of cement. With the increase of cement content, the UCS and ITS values of CSMRA materials increased gradually. For example, compared with the UCS value of 2.88 MPa for C3 group at 7 days, the UCS values for C4, C5, and C6 groups were 3.86, 5.4, and 6.56 MPa, respectively, which signified a corresponding increase of 34.0, 87.5, and 127.8%, respectively. These findings demonstrated that the cement stabilizer was critical for the strength formation of CSMRA materials. Meanwhile, the UCS and ITS values of CSMRA materials exhibited a logarithmic increase trend with age, except for C0 group. Within 7 days, the mechanical strength

of CSMRA materials increased significantly, but the rate of strength increase gradually declined after 7 days.

Figure 8 depicts the relationship between UCS and ITS of CSMRA materials. An almost linear relationship between the UCS (f_c) and ITS (f_{it}) of CSMRA materials could be observed. The linear model was established as $f_{it} = 0.11f_c$, indicating that the ITS of CSMRA materials was approximately 1/9 of the UCS. Previous researchers also reported the linear relationship between UCS and ITS of cement-stabilized natural aggregate materials. The model was expressed as $f_{it} = af_c$, where a was an experimental coefficient with an approximate value of 0.1–0.15 [42,43].

3.2 Stress–strain curve and failure behavior

Figure 9 shows the stress–strain curve for the unconfined compressive and indirect tensile tests of CSMRA materials at 7 days. Three typical stages were observed during compressive and tensile failure processes: (i) compaction stage, when the stress was at a low level, CSMRA materials were gradually compacted tightly; (ii) elastic stage, the stress and strain increased sharply, showing a linear trend; and (iii) yield stage, the stress increased slowly while the strain increased rapidly, resulting in plastic deformation. Previous literature has also found such similar results [44,45].

The ultimate compressive and tensile strains were the vertical and horizontal strains of specimens when the ultimate load was reached. The ultimate compressive strains and tensile strains of C0, C3, C4, C5, and C6 groups were 2.25%, 2.34%, 2.52%, 2.59%, and 2.60% and 0.152%, 0.193%, 0.2%, 0.232%, and 0.235%, respectively. The results indicated that the ultimate compressive and tensile strains of CSMRA materials were gradually increased with the cement content. Because the bonding force between aggregates became stronger with more cement stabilizer content, the CSMRA materials became more deformation resistant when loaded.

Figure 10 depicts a typical failure surface of CSMRA specimens after the indirect tensile test. Tensile failure of CSMRA specimens mainly occurred at the cement mortar attached to aggregates, which was similar to conventional cement-stabilized natural aggregate materials. In particular, parts of brick aggregates and old mortar aggregates were also broken because of tensile damages. This failure occurred because the strengths of some brick aggregates and old mortar aggregates were lower than the overall tensile strength of CSMRA specimens.

3.3 Drying shrinkage

Cement-stabilized materials exhibit drying shrinkage deformation owing to the evaporation of moisture and internal hydration of cement, which may cause shrinkage cracking. Cracks have an adverse effect on cement-stabilized base and severely reduce the service life. In this study, the drying

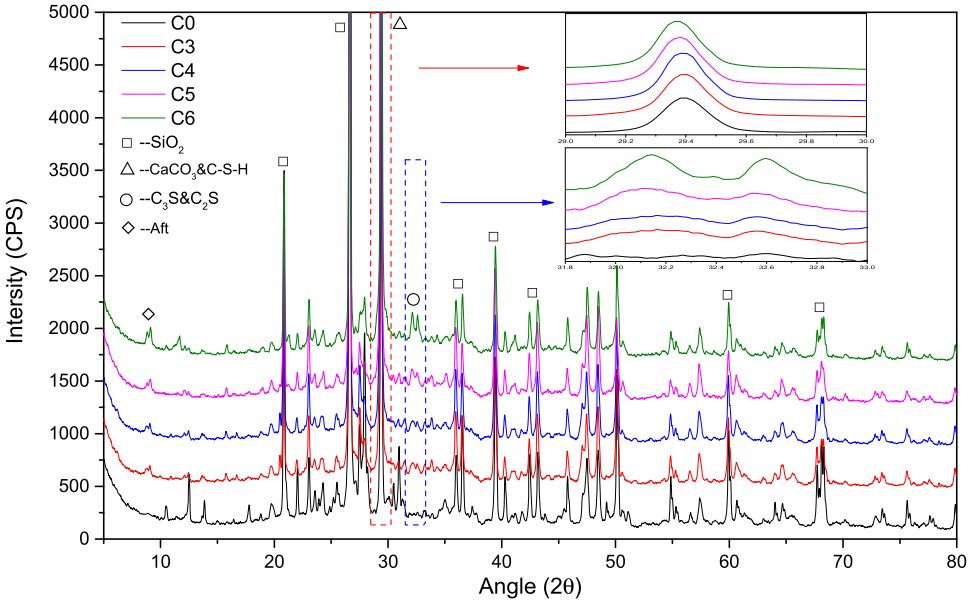

Figure 12: XRD diffraction spectrum of CSMRA materials at 28 days.

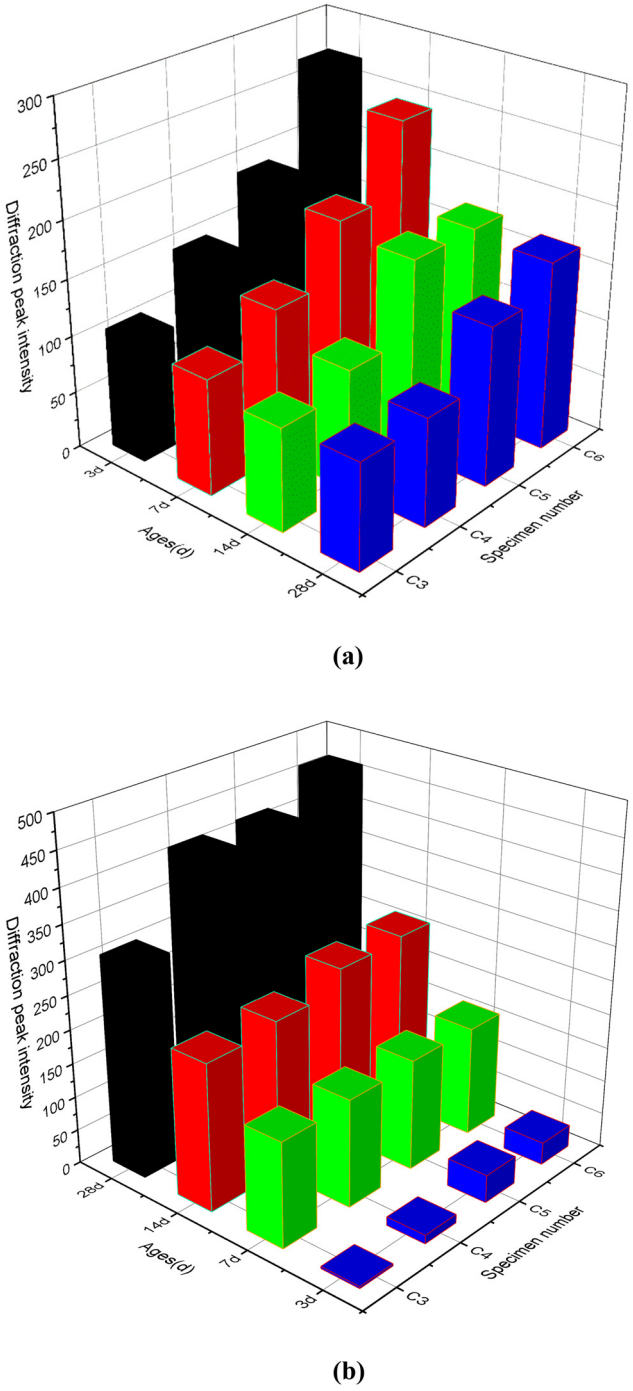

Figure 13: Intensity of (a) C_2S and C_3S and (b) CSH of CSMRA materials with different cement contents.

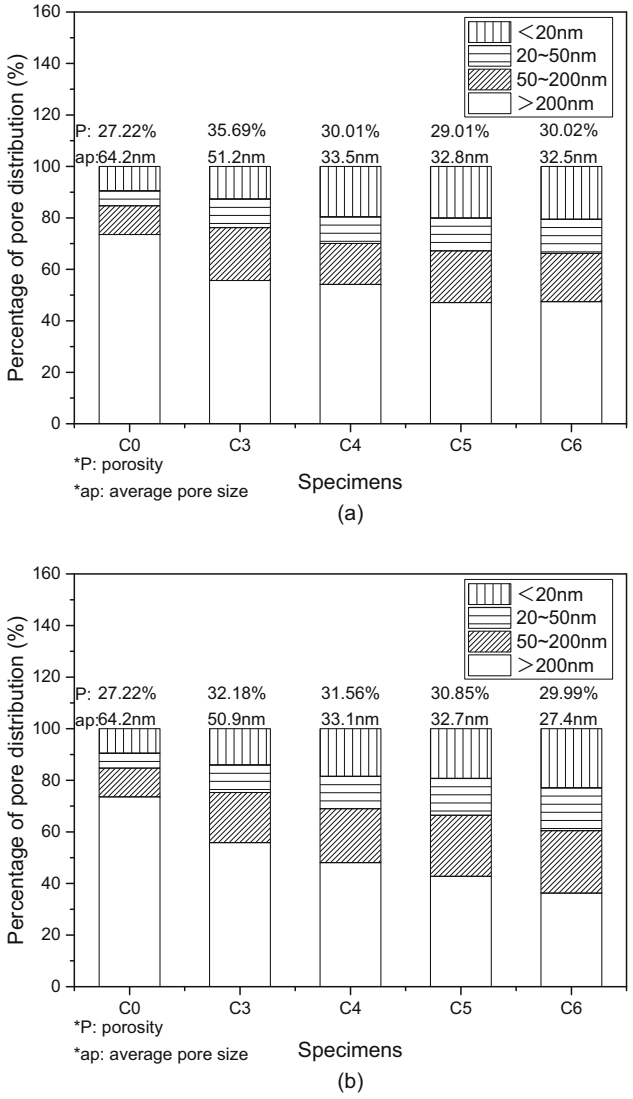

Figure 14: Pore structure distribution of CSMRA materials at (a) 3 days and (b) 28 days.

shrinkage deformation and water loss rate of CSMRA materials within 31 days were determined.

Figure 11 shows the drying shrinkage deformation and water loss rate of CSMRA materials with different cement contents. As the age increased, the drying shrinkage deformation and water loss rate increased gradually. The drying shrinkage deformation of C3, C4, C5, and C6 groups at 31 days were 413.5, 444.7, 531.2, and 606.1 $\mu\varepsilon$, respectively. When the cement content increased from 3 to 4%, the shrinkage deformation increased by 7.5%. When the cement content increased from 4 to 5%, the shrinkage deformation increased by 19.4%. When the cement content increased from 5 to 6%, the shrinkage deformation increased by 14.1%. It indicated that higher cement content would cause extensive drying shrinkage deformation and the drying shrinkage deformation increased sharply when the cement content exceeded 4%. However, the water loss rate of CSMRA materials decreased with the cement content. The water loss rate of C3, C4, C5, and C6 groups at 31 days were 13.11, 12.78, 12.3, and 11.89%, respectively, possibly because more water was involved in the cement hydration reaction and less water was

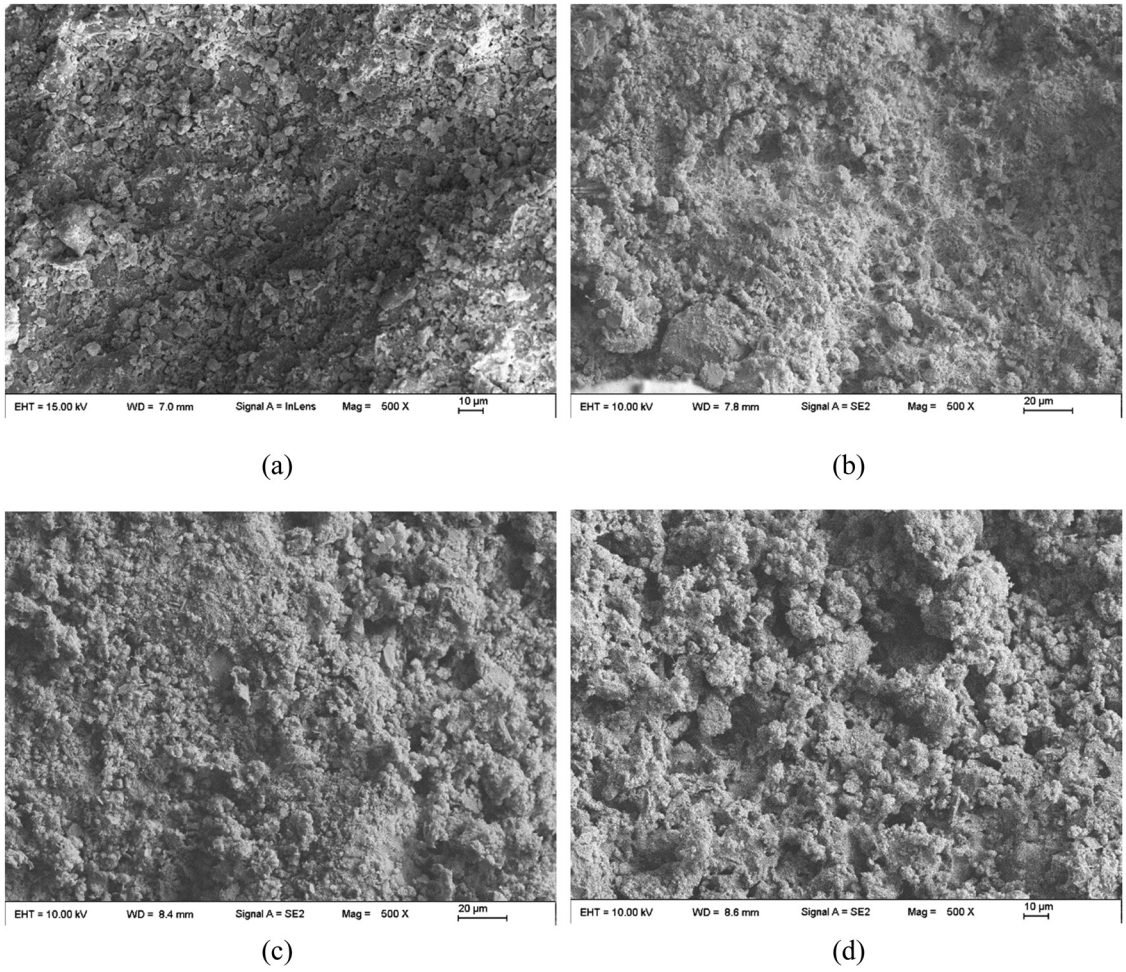

Figure 15: Micromorphology comparison of CSMRA materials with different cement contents (28 days): (a) C0, (b) C3, (c) C4, and (d) C5.

lost during the drying process when the cement content increased.

3.4 XRD analysis

Figure 12 depicts the XRD diffraction spectrum of CSMRA materials at 28 days. The major phases of C0 group without cement stabilizer were quartz (SiO_2) and limestone ($CaCO_3$), derived from the MRA. While the main phases of C3, C4, C5, and C6 groups contained cement clinker minerals (C_2S and C_3S) and cement hydration products (CSH and Aft). The peaks at $2\theta = 32.2°$ and 32.6° and $2\theta = 29.4°$ were adopted as the characteristic peaks of C_2S and C_3S and $CaCO_3$ and CSH, respectively, and the peak intensity was obtained according to the semi-quantitative method.

Figure 13 shows the intensity of C_2S and C_3S and CSH (the peak intensity of $CaCO_3$ of C0 group was deducted) of CSMRA materials with different cement contents. It could be seen that the intensity of C_2S&C_3S gradually decreased with age, while the intensity of CSH gradually increased with age. The cement clinker mineral in CSMRA materials was hydrated and consumed to form more hydration product CSH. Moreover, the intensity of CSH increased faster during the early stage, which was consistent with the developmental trend of mechanical strength.

3.5 Pore structure analysis

Figure 14 depicts the pore structure distribution of CSMRA materials at 3 days and 28 days. Results indicated that the specimens of C0 group had the largest average pore sizes and 73.6% harmful pores (>200 nm). While the porosity and the average pore size of C3, C4, C5, and C6 groups decreased gradually, the proportion of harmful pores decreased and the proportion of harmless pores

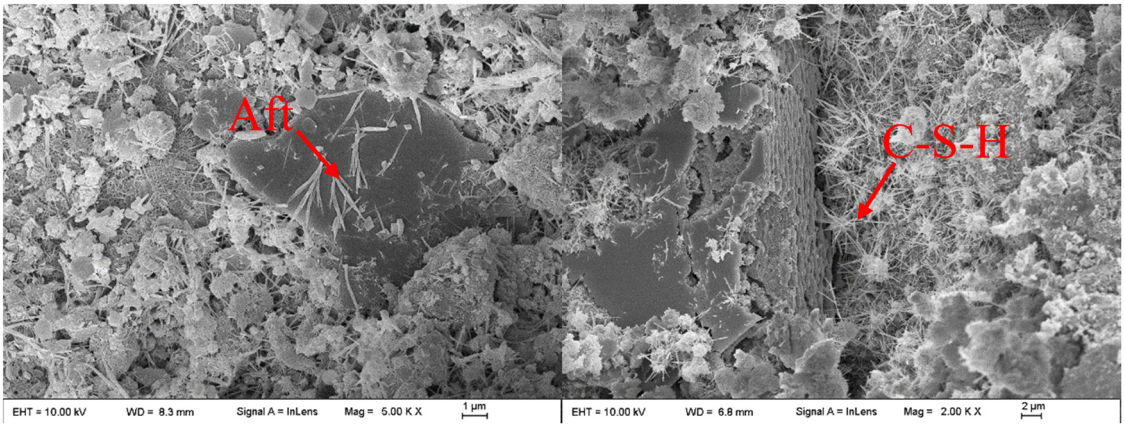

Figure 16: Micromorphology of CSMRA materials at 28 days (C6 group).

(<20 nm) increased. These findings indicated that cement had a filling effect on CSMRA materials, which reduced the porosity and optimized the pore structure distribution. By comparing the pore structure distribution of CSMRA materials at 3 days with those at 28 days, it could be found that the porosity and the average pore size of CSMRA material showed a decreasing trend. CSH gel produced by the hydration of cement could fill the micropores between aggregates and optimize the pore distribution of CSMRA materials.

3.6 Micromorphology observation

Figure 15 shows the micromorphology comparison of CSMRA materials with different cement contents at the age of 28 days. With the increase of the cement content, more hydration products could be seen. Figure 16 depicts the micromorphology of CSMRA materials at 28 days. Flocculent CSH, needle-shaped Aft, and aggregates attached and wrapped by cement hydration products could be observed. It was consistent with the XRD phase analysis results. Precisely because of the binding force and the filling effect between aggregates of these hydration products, the CSMRA materials can develop certain strength to resist load and deformation.

4 Conclusion

In this study, 100% MRA was used to prepare cement-stabilized materials as road base. The mechanical properties and microstructures of CSMRA materials were systematically examined through strength tests, drying shrinkage tests, XRD, MIP, and SEM. Based on the findings of the study, the following conclusions are mainly drawn:

(1) Using 100% MRA to prepare cement-stabilized materials was feasible. Cement-stabilized MRA materials exhibited satisfactory mechanical performance in terms of UCS, ITS, and drying shrinkage deformation.
(2) Cement was the basis for the strength formation of CSMRA materials. The UCS and ITS of the CSMRA materials gradually increased with age owing to the continuous hydration of cement. Due to the low content of cement, the mechanical strength of the CSMRA materials significantly increased within 7 days, but the rate of strength increases gradually declined after 7 days.
(3) The UCS and ITS of CSMRA materials increased with the cement content. An approximately linear relationship between the UCS and ITS of CSMRA materials was established as $f_{it} = 0.11\, f_c$.
(4) Three typical stages of CSMRA materials were observed during the compressive and tensile failure processes: (i) compaction stage, (ii) elastic stage, and (iii) yield stage. The ultimate compressive and ultimate tensile strains of CSMRA materials increased with the cement content. In addition, part of the brick aggregates and old mortar aggregates were destroyed by tensile damages.
(5) The use of a higher cement content would result in a larger drying shrinkage deformation and less water loss of CSMRA materials owing to the evaporation of moisture and internal hydration of cement. The drying shrinkage deformation of the CSMRA materials increased sharply when the cement content exceeded 4%. When using 100% MRA to prepare cement-stabilized materials, it is necessary to pay more attention to its drying shrinkage deformation.

(6) Cement has both filling and binding effects on CSMRA materials. The CSH gel produced by the hydration of the cement clinker minerals C_2S and C_3S acted as a binder for MRA. It could also fill the micropores and optimize the pore structure distribution of CSMRA materials.

The results demonstrate the feasibility of using 100% MRA in cement-stabilized materials, which will significantly enhance the utilization efficiency of MRA in road engineering.

Funding information: This study was supported by the Bilateral Zhejiang-West Flanders Industrial R&D Project of Zhejiang Key Research & Development Program (2020C04013) and Hangzhou Qianjiang New City Municipal Garden Construction Co., Ltd.

Author contributions: Conceptualization, writing – review & editing, supervision, project administration, funding acquisition, T.M.; methodology, formal analysis, writing – original draft, S.L.; validation, K.Y.; investigation, H.Y.

Conflict of interest: Authors state no conflict of interest.

References

[1] Wu, Z., A. T. W. Yu, L. Shen, and G. Liu. Quantifying construction and demolition waste: An analytical review. *Waste Management*, Vol. 34, No. 9, 2014, pp. 1683–1692.

[2] Ajayi, S. O., L. O. Oyedele, O. O. Akinade, M. Bilal, H. A. Owolabi, H. A. Alaka, et al. Reducing waste to landfill: A need for cultural change in the UK construction industry. *Journal of Building Engineering*, Vol. 5, 2016, pp. 185–193.

[3] Zheng, L., H. Wu, H. Zhang, H. Duan, J. Wang, W. Jiang, et al. Characterizing the generation and flows of construction and demolition waste in China. *Construction and Building Materials*, Vol. 136, 2017, pp. 405–413.

[4] Silva, R. V., J. de Brito, C. J. Lynn, and R. K. Dhir. Environmental impacts of the use of bottom ashes from municipal solid waste incineration: A review. *Resources, Conservation And Recycling*, Vol. 140, 2019, pp. 23–35.

[5] Van Praagh, M. and H. Modin. Leaching of chloride, sulphate, heavy metals, dissolved organic carbon and phenolic organic pesticides from contaminated concrete. *Waste Management*, Vol. 56, 2016, pp. 352–358.

[6] Lee, J. Y., S. H. Moon, M. J. Yi, and S. T. Yun. Groundwater contamination with petroleum hydrocarbons, chlorinated solvents and high pH: Implications for multiple sources. *Quarterly Journal of Engineering Geology and Hydrogeology*, Vol. 41, No. 1, 2008, pp. 35–47.

[7] Vouk, D., D. Nakic, N. Stirmer, and C. R. Cheeseman. Use of sewage sludge ash in cementitious materials. *Reviews on Advanced Materials Science*, Vol. 49, No. 2, 2017, pp. 158–170.

[8] Bravo, M., J. de Brito, J. Pontes, and L. Evangelista. Durability performance of concrete with recycled aggregates from construction and demolition waste plants. *Construction and Building Materials*, Vol. 77, 2015, pp. 357–369.

[9] Bravo, M., J. de Brito, J. Pontes, and L. Evangelista. Mechanical performance of concrete made with aggregates from construction and demolition waste recycling plants. *Journal of Cleaner Production*, Vol. 99, 2015, pp. 59–74.

[10] Badur, S. and R. Chaudhary. Utilization of hazardous wastes and by-products as a green concrete material through S/S process: A review. *Reviews on Advanced Materials Science*, Vol. 17, No. 1, 2008, pp. 42–61.

[11] Sormunen, P. and T. Karki. Recycled construction and demolition waste as a possible source of materials for composite manufacturing. *Journal of Building Engineering*, Vol. 24, 2019, id. 100742.

[12] Kumar, R. Influence of recycled coarse aggregate derived from construction and demolition waste (CDW) on abrasion resistance of pavement concrete. *Construction and Building Materials*, Vol. 142, 2017, pp. 248–255.

[13] Kou, S., C. Poon, and H. Wan. Properties of concrete prepared with low-grade recycled aggregates. *Construction and Building Materials*, Vol. 36, 2012, pp. 881–889.

[14] Medina, C., W. Zhu, T. Howind, M. Frias, and M. I. Sanchez De Rojas. Effect of the constituents (asphalt, clay materials, floating particles and fines) of construction and demolition waste on the properties of recycled concretes. *Construction and Building Materials*, Vol. 79, 2015, pp. 22–33.

[15] Li, X. P. Recycling and reuse of waste concrete in China: Part II. Structural behaviour of recycled aggregate concrete and engineering applications. *Resources, Conservation & Recycling*, Vol. 53, No. 3, 2009, pp. 107–112.

[16] Ossa, A., J. L. Garcia, and E. Botero. Use of recycled construction and demolition waste (CDW) aggregates: A sustainable alternative for the pavement construction industry. *Journal of Cleaner Production*, Vol. 135, 2016, pp. 379–386.

[17] Ding, Z., Y. Wang, and P. X. W. Zou. An agent based environmental impact assessment of building demolition waste management: Conventional versus green management. *Journal of Cleaner Production*, Vol. 133, 2016, pp. 1136–1153.

[18] Meng, T., J. L. Zhang, H. D. Wei, and J. J. Shen. Effect of nano-strengthening on the properties and microstructure of recycled concrete. *Reviews on Advanced Materials Science*, Vol. 9, No. 1, 2020, pp. 79–92.

[19] Lopez Ruiz, L. A., X. Roca Ramon, and S. Gasso Domingo. The circular economy in the construction and demolition waste sector – a review and an integrative model approach. *Journal of Cleaner Production*, Vol. 248, 2020, id. 119238.

[20] Wu, H., J. Wang, H. Duan, L. Ouyang, W. Huang, and J. Zuo. An innovative approach to managing demolition waste via GIS (geographic information system): A case study in Shenzhen city, China. *Journal of Cleaner Production*, Vol. 112, No. 1, 2016, pp. 494–503.

[21] Xuan, D. X., L. J. M. Houben, A. A. A. Molenaar, and Z. H. Shui. Mechanical properties of cement-treated aggregate material – a review. *Material and Design*, Vol. 33, 2012, pp. 496–502.

[22] Paria, S. and P.K. Yuet. Solidification-stabilization of organic and inorganic contaminants using portland cement:

A literature review. *Environmental Reviews*, Vol. 14, No. 4, 2006, pp. 217–255.
[23] Parreira, A. B., A. Kobayashi, and O. B. Silvestre. Influence of portland cement type on unconfined compressive strength and linear expansion of cement-stabilized phosphogypsum. *Journal of Environmental Engineering*, Vol. 129, No. 10, 2003, pp. 956–960.
[24] Poon, C. S. and D. Chan. Feasible use of recycled concrete aggregates and crushed clay brick as unbound road sub-base. *Construction and Building Materials*, Vol. 20, No. 8, 2006, pp. 578–585.
[25] Gabr, A. R. and D. A. Cameron. Properties of recycled concrete aggregate for unbound pavement construction. *Journal of Materials in Civil Engineering*, Vol. 24, No. 6, 2012, pp. 754–764.
[26] Saberian, M., J. Li, M. Boroujeni, D. Law, and C. Q. Li. Application of demolition wastes mixed with crushed glass and crumb rubber in pavement base/subbase. *Resources, Conservation And Recycling*, Vol. 156, 2020, id. 104722.
[27] Disfani, M. M., A. Arulrajah, H. Haghighi, A. Mohammadinia, and S. Horpibulsuk. Flexural beam fatigue strength evaluation of crushed brick as a supplementary material in cement stabilized recycled concrete aggregates. *Construction and Building Materials*, Vol. 68, 2014, pp. 667–676.
[28] Azam, A. M. and D. A. Cameron. Geotechnical properties of blends of recycled clay masonry and recycled concrete aggregates in unbound pavement construction. *Journal of Materials in Civil Engineering*, Vol. 25, No. 6, 2013, pp. 788–798.
[29] Xuan, D. X., A. A. A. Molenaar, and L. J. M. Houben. Evaluation of cement treatment of reclaimed construction and demolition waste as road bases. *Journal of Cleaner Production*, Vol. 100, 2015, pp. 77–83.
[30] Leite, F. D. C., R. D. S. Motta, K. L. Vasconcelos, and L. Bernucci. Laboratory evaluation of recycled construction and demolition waste for pavements. *Construction and Building Materials*, Vol. 25, No. 6, 2011, pp. 2972–2979.
[31] Mohammadinia, A., A. Arulrajah, J. Sanjayan, M. M. Disfani, M. W. Bo, and S. Darmawan. Laboratory evaluation of the use of cement-treated construction and demolition materials in pavement base and subbase applications. *Journal of Materials in Civil Engineering*, Vol. 27, 2015, id. 040141866.
[32] Mohammadinia, A., P. R. Oskooei, and A. Arul. Discrete element modeling of cemented recycled concrete aggregates under unconfined and k_0 loading conditions. *Transportation Geotechnics*, Vol. 10, No. 1, 2020, id. 100450.
[33] Hou, Y., X. Ji, and X. Su. Mechanical properties and strength criteria of cement-stabilized recycled concrete aggregate. *International Journal of Pavement Engineering*, Vol. 20, No. 3, 2019, pp. 339–348.
[34] Xuan, D. X., L. J. M. Houben, A. A. A. Molenaar, and Z. H. Shui. Mixture optimization of cement treated demolition waste with recycled masonry and concrete. *Materials and Structures*, Vol. 45, No. 1–2, 2012, pp. 143–151.
[35] Xuan, D. X., E. Schlangen, A. A. A. Molenaar, and L. J. M. Houben. Influence of quality and variation of recycled masonry aggregates on failure behavior of cement treated demolition waste. *Construction and Building Materials*, Vol. 71, 2014, pp. 521–527.
[36] Xuan, D. X., A. A. A. Molenaar, and L. J. M. Houben. Deformation behavior of cement treated demolition waste with recycled masonry and concrete subjected to drying and temperature change. *Cement and Concrete Composite*, Vol. 68, 2016, pp. 27–34.
[37] Jia, X., F. Ye, and B. Huang. Utilization of construction and demolition wastes in low-volume roads for rural areas in China. *Transportation Research Record*, Vol. 2474, 2015, pp. 39–47.
[38] Agrela, F., A. Barbudo, A. Ramirez, J. Ayuso, M. Dolores Carvajal, and J. Ramon Jimenez. Construction of road sections using mixed recycled aggregates treated with cement in Malaga, Spain. *Resources, Conservation And Recycling*, Vol. 58, 2012, pp. 98–106.
[39] Perez, P., F. Agrela, R. Herrador, and J. Ordonez. Application of cement-treated recycled materials in the construction of a section of road in Malaga, Spain. *Construction and Building Materials*, Vol. 44, 2013, pp. 593–599.
[40] JTG D50. *Specifications for design of highway asphalt pavement*, China Communication Press Co., Ltd, Beijing, China, 2017.
[41] JTG E51. *Test methods of materials stabilized with inorganic binders for highway engineering*, China Communication Press Co., Ltd, Beijing, China, 2009.
[42] Kolias, S. and R. I. T. Williams. Relationships between the static and the dynamic moduli of elasticity in cement stabilized materials. *Materials Construction*, Vol. 13, No. 2, 1980, pp. 99–107.
[43] Babić, B. Relationships between mechanical properties of cement stabilized materials. *Materials and Structures*, Vol. 20, No. 6, 1987, pp. 455–460.
[44] Saberian, M., J. Li, and D. Cameron. Effect of crushed glass on behavior of crushed recycled pavement materials together with crumb rubber for making a clean green base and subbase. *Journal of Materials in Civil Engineering*, Vol. 31, 2019, id. 040191087.
[45] Arulrajah, A., M. M. Disfani, H. Haghighi, A. Mohammadinia, and S. Horpibulsuk. Modulus of rupture evaluation of cement stabilized recycled glass/recycled concrete aggregate blends. *Construction and Building Materials*, Vol. 84, 2015, pp. 146–155.